https://doi.org/10.15407/ujpe65.3.225

J.I. HUSEYNOV,[1] KH.A. HASANOV,[1] T.A. JAFAROV,[1] I.I. ABBASOV[2]

[1] Azerbaijan State Pedagogical University
(AZ1000, Baku 68, Uzeyir Hajibeyli str., Baku, Azerbaijan; e-mail: cahangir.adpu@mail.ru)
[2] Azerbaijan State University of Oil and Industry
(Baku, Azerbaijan)

COMPENSATING EFFECT OF TERBIUM IMPURITY ON THE CONDUCTIVITY OF $Tb_xSn_{1-x}Se$ SOLID SOLUTIONS

The interactions in the SnSe–TbSe system are investigated, and the solubility region of TbSe in SnSe is determined from the results of a complex physicochemical analysis. The dependence of the electrical conductivity and the concentration of current carriers of $Tb_xSn_{1-x}Se$ crystals on the composition and temperature is analyzed.

Keywords: chalcogenides, solid solutions, electrical conductivity, Hall coefficient, valence band, light and heavy holes.

1. Introduction

The active development of the electronic technology requires the creation and study of new semiconductor materials with improved properties compared with traditional semiconductors. Such materials include the rare-earth semiconductors, whose properties are associated with the uniqueness of the electronic structure. The peculiarity of the electronic structure of rare-earth elements is the filling of the 4f-shell with an unfilled d shell [1, 2].

The electron configuration of rare-earth metal (REM) ions is based on the xenon structure $1s^2 2s^2 2p^6 3s^2 3p^6 3d^{10} 4s^2 4p^6 4d^{10} 5s^2 5p^6$ and, above it, electrons on a partially filled 4f-shell and two or three external electrons ($6s^2$ or $5d6s^2$). The 4f-shells are rather compact and well shielded by closed 5s5p-shells which are located close to them, so the direct overlap of the electrons of neighboring ions is negligible. The outermost 6s6p5d-electrons form a conduction band, leaving rare-earths in a solid trivalent. The properties of this band determine their electrical and optical properties and transport phenomena.

Tin monoselenide is one of the chalcogenide layered semiconductors of the $A^{IV}B^{VI}$ group, whose unique properties, in particular, the high chemical stability, high absorption coefficient, as well as the value of the band gap of 1–1.5 eV (covers the visible and near infrared region) and stable p-type conductivity with the development of photovoltaics, attract more and more attention [3–5]. Doping them with impurities that create quasilocal levels expands the possibilities of their practical application. The electronic configuration, chemical activity, atomic and ionic radii, and REM make them most suitable as a ligator for tin monoselenide.

The introduction of REM into tin monoselenide leads to the formation of a number of physical features associated with the nature of the defect formation and with the interaction of defects. Therefore, the study of the interaction between SnSe and TbSe chalcogenides, as well as a comprehensive study of charge transfer processes in the formed solid solutions, is of scientific and practical interest for the cre-

© J.I. HUSEYNOV, KH.A. HASANOV, T.A. JAFAROV, I.I. ABBASOV, 2020

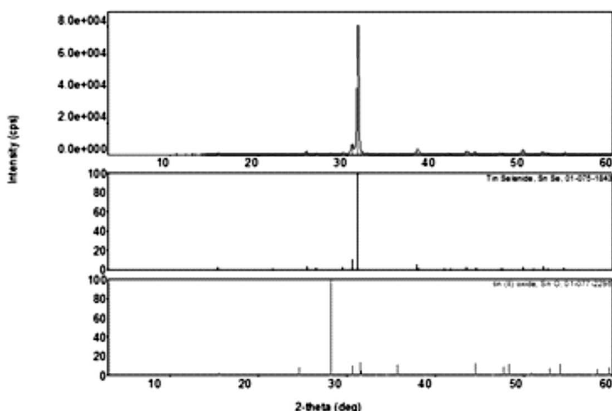

Fig. 1. X-ray diffraction pattern for $Tb_xSn_{1-x}Se$ with $x = 0.0025$. Samples of SnSe and SnO are shown below

ation of some electrical energy converters and various thermistors resistant to radiation, pressure, and humidity. Below, we will present the results of studies of the dependence of the electrical conductivity and the Hall coefficient on the temperature, as well as the dependence of these parameters on the concentration of terbium in the $Tb_xSn_{1-x}Se$ solid solution.

2. Experimental Technique

The initial components, namely, tin of "B4-000" brand, selenium of "OC417-4" brand, and chemically pure terbium (99.98%), were used for the synthesis of alloys of the SnSe–TbSe system. The synthesis was carried out in an evacuated quartz ampoule at a pressure of 0.1333 Pa by the method of direct melt of the components in two stages. Samples of the solid solution of $(SnSe)_{1-x}$–$(TbSe)_x$ with the composition of $x_1 = 0.0025$; $x_2 = 0.005$; $x_3 = 0.02$; $x_4 = 0.03$, and $x_5 = 0.04$ were synthesized. At the initial stage, the ampoule together with the substance was heated up to the melting point of selenium at a rate of 4–5 degree/minute and held at this temperature for 3–4 hours. Then the temperature was gradually increased up to 950–1000 °C depending on the composition and held for 8–9 hours.

For the complex physicochemical analysis and electrophysical studies, the synthesized samples were annealed for 100–140 hours depending on the composition: the annealing time was increased with the content of terbium. The homogenizing annealing of the obtained single-phase samples was carried out in a medium of spectrally pure argon at 800 K. Single crystals were grown by the Bridgman method.

The structure, phase, and elemental composition of the obtained ingots and the state of the surface along the plane of the natural layers of the studied samples were determined by conducting complex X-ray diffraction, radiographic, thermographic, X-ray spectroscopy, and microscopic analyses.

DTA was performed on a Perkin Elmer STA 6000 (USA) in order to determine the thermal effects of the obtained samples and the phase transitions. Nitrogen with a feed rate of 20 ml/s was used as the working gas; the sample was heated up to the melting at a heating rate of 5 °C/min.

X-ray diffraction analysis was performed on an X-ray diffractometer Miniflex by "Rigaku Corporation" on 30 kV mode, 10 mA, radiation $CuK_\alpha(\lambda = 1.5406$ Å). Diffraction reflections were observed at a step of 0.01° and a displacement angle of 2θ in the range of $0-80°$. A Japanese-made scanning electron microscope of JEOL JSM6610-LV brand was used for the study of a morphology and a microcomposition of the sample surface.

After the annealing, samples $2 \times 4 \times 18$ mm^3 in size were cut out from the ingots of crystals in an electrospark installation. The electrical conductivity and the Hall coefficient were measured at a constant current and a constant magnetic field of an electromagnet [6]. The thermal electromotive force was measured by a stationary method according to the method described in [7]. The measurements were carried out in the temperature range of 80÷350 K. The experimental error did not exceed 4.2%.

3. Results and Discussion

Besides the thermal effect corresponding to the melting, no other thermal effects are observed on the thermograms of the $Tb_xSn_{1-x}Se$ alloy system. In the SnSe binary compound, the partial replacement of Sn atoms by Tb atoms helps to reduce the melting temperature. The results of complex physicochemical analysis show that the system of $Tb_xSn_{1-x}Se$ alloys, as well as the main substance SnSe, crystallizes in the orthorhombic system with the space group $D_{2h}^{16} - P_{cmn}$ (Fig. 1). With an increase in the percentage of TbSe in the composition, a slight increase in the unit cell parameters of the crystal lattice, density, and microhardness is observed, and the heat effects

shift to relatively lower temperatures. In all compositions, the density calculated on the basis of radiographic data is higher than the density determined by the pycnometric method. This shows that the obtained system of alloys is rich in defects consisting of vacancies of structural elements.

Figure 2, *a* shows a two-dimensional image obtained as a result of an increase in the surface area of $5 \times 10^3 \times 5 \times 10^3$ with respect to homogeneous $Tb_xSn_{1-x}Se$ single crystals using an atomic force microscope. In Fig. 2, *b*, a volumetric image of a part with a relatively uniform surface relief of the same single crystal is given. As it can be seen from the figure, the $Tb_xSn_{1-x}Se$ single crystal surface is sufficiently uniform and even.

Despite the fact that SnSe single crystals are layered crystals, some roughness is observed on the natural cleavage surface. A histogram analysis of the images obtained by an atomic force microscope shows that the natural uniformity of the surface of the SnSe single crystal varies within 25 nm. The observation of a certain roughness in the near-boundary layer is most likely due to the presence of weak van der Waals forces between the layers; when the bonding forces are destroyed, not individual atoms, but clusters of atoms remain on the surface of the crystal [8].

The surface roughness also increases with the number of REM in the $Tb_xSn_{1-x}Se$ single crystal. In the SnSe binary compound, the partial replacement of Sn atoms by the rare-earth metal atoms with a greater radius leads to an increase in the weak van der Waals bond between the layers. Therefore, with an increase in the amount of Tb in the composition of the $Tb_xSn_{1-x}Se$ alloy system, the layer-by-layer rejection becomes more complex, and the roughness of the natural surface increases. The Fourier spectrum obtained by atomic force microscopy also shows this. Surface particles located mainly at the center of the image of the spectrum have approximately the same size.

The observed growth of the lattice parameters, good agreement of the partial replacement of Sn atoms by Tb atoms of a larger radius, and the observance of Vegard's law suggest the formation of substitution solid solutions based on SnSe. The study of the dependence of the microstructure, microhardness, and density of the composition detected by the X-ray and pycnometric methods shows that the region of dissolution of TbSe in SnSe at room temperature is limited to 4 mol%.

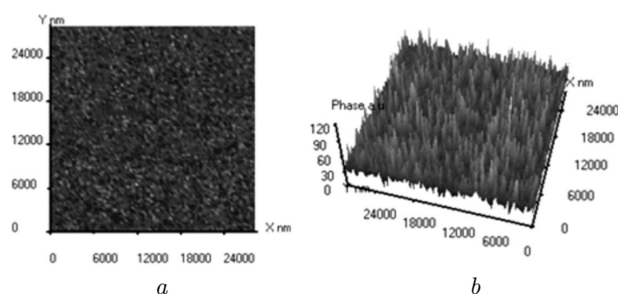

Fig. 2. AFM image of the $Tb_xSn_{1-x}Se$ single crystal surface: two-dimensional (*a*) and volume (*b*)

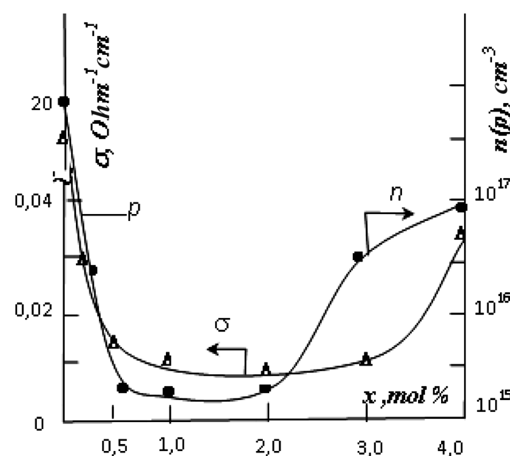

Fig. 3. Dependence of the electroconductivity and concentration of current carriers of $Tb_xSn_{1-x}Se$ crystals on the composition

Figure 3 shows the dependence of the specific electroconductivity and the concentration of current carriers on the amount of terbium contained in the $Tb_xSn_{1-x}Se$ alloy. At low concentrations, the specific electroconductivity decreases, as the amount of Tb in the system of $Tb_xSn_{1-x}Se$ alloys increases, whereas an increase in conductivity at $x > 0.02$ is observed. The value of the thermal electromotive force coefficient decreases with increasing the terbium concentration and changes its sign from p to n-type at $x \geq 0.001$ and then stabilizes, by passing through a maximum in absolute value in solid solutions $Tb_xSn_{1-x}Se$.

At concentrations of Tb $0 \leq x \leq 0.01$, the filling of tin vacancies and a change in chalcogenic antistructural defects lead to a decrease in the concentration of charge carriers and in the specific electroconductivity. It can be said that, with a subsequent increase in the amount of TbSe, no antistructural defects are cre-

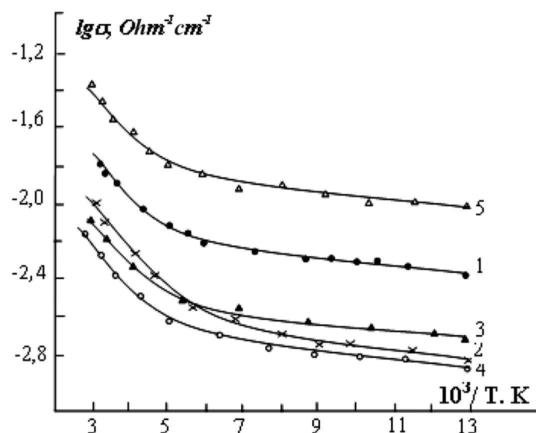

Fig. 4. Dependence of the electroconductivity of $Tb_xSn_{1-x}Se$ crystals on the temperature: 0.25 (*1*); 0.5 (*2*); 2 (*3*); 3 (*4*); 4 mol% (*5*)

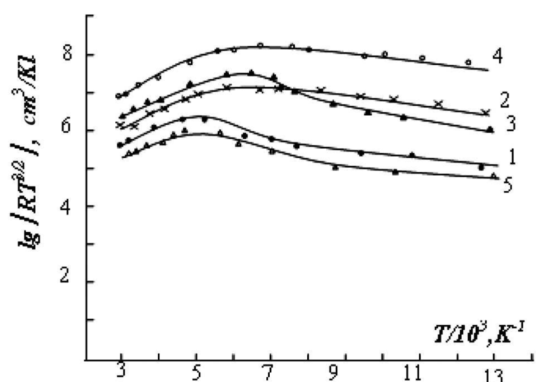

Fig. 5. Dependence of the Hall coefficient of $Tb_xSn_{1-x}Se$ on the temperature: 0.25 (*1*); 0.5 (*2*); 2 (*3*); 3 (*4*); 4.0 mol% (*5*)

Dependence of activation energies (eV) on the composition

Ingredients, mol%	Electrical conductivity		Hall coefficient	
	E_{a1}	E_{a2}	E_{a1}	E_{a2}
0.25	0.026	0.130	0.025	0.128
0.5	0.024	0.125	0.023	0.124
2.0	0.022	0.123	0.022	0.122
3.0	0.022	0.122	0.021	0.120
4.0	0.020	0.121	0.021	0.120

ated. We assume that a partial increase in the specific electrical conductivity is associated with the appearance of the second kind of charge carriers, as a result of the action of donor Tb atoms. However, since tin with chalcogen is bivalent in SnSe, its partial substitution by trivalent terbium appears to result in the appearance of shallow donor levels due to the participation of a tin vacancy. The indicated features of the experimental data indicate the occurrence of the self-compensation in $Tb_xSn_{1-x}Se$.

The agreement of the experiment with the theory can be attained, if it is assumed that the doping with the Tb impurity is compensated not only by vacancies, but also by the formation of complexes. The self-compensation model, which accounts for the possibility of the formation of complexes of a terbium impurity ion – a tin vacancy, describes the self-compensation in the $Tb_xSn_{1-x}Se$ alloy.

The doping of semiconductor materials leads to the occurring of impurity levels in the energy spectrum of charge carriers. An important parameter characterizing the impurity center is the activation energy E_a (the energy necessary to tear the electron from the center). In accordance with the value of E_a, impurity levels can be divided into shallow and deep. For shallow impurity centers, the ionization energy is much less than the band gap width ($E_a \ll E_g$). Some impurities create deep impurity levels in semiconductors located far from the boundaries of energy bands. Atoms of transition metals (as well as REM), which have unfilled spaces on the internal electron shells, give deep local levels in almost all known semiconductor materials.

Figure 4 shows the temperature dependence of the specific electrical conductivity of single crystals grown from the system of $Tb_xSn_{1-x}Se$ alloys. As is seen from the figure, the specific electrical conductivity in the temperature range 80–350 K for the studied crystals is inherent to classical semiconductors. At low temperatures, there is a weak dependence of the electrical conductivity on the temperature. At temperatures $T < 180$ K, the electrical conductivity can be considered the impurity conductivity resulting from the transfer of charge carriers under the thermal excitation from a level localized near the Fermi one to a delocalized level located in the conduction band. With an increase in the amount of Tb in the composition, a decrease in the activation energy of charge carriers is observed.

Starting from a temperature of 200 K, the conductivity increases sharply, since the electrons of the valence band, which absorb the energy equal or greater

than the activation energy of deep impurities, pass into the conduction band and participate in the electrical conductivity. The activation energy of impurity centers was determined based on the tendency of the dependence $\lg\sigma = f\left(\frac{10^3}{T}\right)$ to the low-temperature and high-temperature regions, the results of which are shown in Table. As can be seen from the table in the low-temperature and high-temperature regions, the activation energy of charge carriers at impurity levels is $E_{a1} \approx 0.02$ eV and $E_{a2} \approx 0.12$ eV, respectively.

By a partial replacement of Sn atoms by Tb atoms in the SnSe crystal lattice with an increase in the number of REEs, there is a slight tendency to a decrease in the band gap. The cause for this is the elementary growth of lattice parameters due to the partial replacement of Sn atoms with an ionic radius of 0.67 Å with lanthanide atoms of even larger radii (≈1 Å) [9]. With an increase in the terbium impurity concentration in $Tb_xSn_{1-x}Se$ single crystals, the deformed state increases, and, as a result, the conductivity and mobility of charge carriers decrease.

Figure 5 shows the temperature dependences of the Hall coefficient of the system of $Tb_xSn_{1-x}Se$ alloys in the coordinates $\lg\left(RT^{3/2}\right) \infty \frac{10^3}{T}$, which makes it possible to determine the band parameters. The results are presented in Table. According to the analysis of the dependence of the Hall coefficient on the temperature for single crystals $(SnSe)_{1-x}(TbSe)_x$ in the region of impurity conductivity starting from the boiling point of nitrogen to a temperature of 240 K, remaining unchanged, we can say that it does not depend on the temperature. With a subsequent increase in the temperature (250–350 K), the Hall coefficient increases. This anomaly is explained by the presence of traps in the band gap for electrons or by the formation of additional acceptors with increasing the temperature [6].

In the presence of light and heavy holes, due to the weak dependence, the ratio of the hole mobilities of the main and additional extrema of the valence band, the temperature dependence ofthe Hall coefficient is determined by the distribution of charge carriers in the valence subbands. As the temperature increases, an increasing number of holes goes into subbands, and the effective concentration of holes participating in the conductivity decreases. Due to the weak mobility of holes in the second valence band, their fraction in the Hall effect is weak, due to the passage of holes into the second band, the effective concentration decreases, and the Hall coefficient increases. With increasing the temperature in the field of intrinsic conductivity, the Hall coefficient decreases sharply. This type of dependence is found in the basic SnSe compound, as well as in its structural counterparts. The cause for this is the complex nature of the band structure of these compounds, the state of the valence band of the two lower zones, and it is explained by the existence of light and heavy holes, respectively.

As can be seen from Figs. 4 and 5, the nature of a change in the dependence of the specific electroconductivity and the Hall coefficient on the temperature is the same for all the studied crystals. It should be noted that the value of the width of the forbidden zone determined from the temperature dependence of the Hall coefficient coincides well with the value determined from data on the specific electroconductivity.

4. Conclusion

The dissolution of TbSe in SnSe at room temperature is limited to 4 mol%. In the system of $Tb_xSn_{1-x}Se$ alloys at terbium concentrations x$\leqslant$0.01, the filling of tin vacancies and a change in chalcogenic antistructural defects lead to a decrease in the electrical conductivity, charge carrier concentration, activation energy, and band gap. The temperature dependence of the Hall coefficient is well explained on the basis of a two-band model.

1. V. Dierolf, I.T. Ferguson, J.M. Zavada. *Rare Earth and Transition Metal Doping of Semiconductor Materials: Synthesis, Magnetic Properties and Room Temperature Spintronics* (Woodhead, 2016).
2. N.V. Kudrevatykh, A.S. Volegov. *Physics of Metals. Rare-Earth Metals and Their Compounds* (Yurayt, 2019) (in Russian).
3. N.R. Mathews. Electrodeposited tin selenide thin films for photovoltaic applications. *Sol. Energy* **86**, 4 (2012).
4. V.R.M. Reddy, S. Gedi, B. Pejjai, C. Park. Perspectives on SnSe-based thin film solar cells: A comprehensive review. *Mater. in Electron.* **27**, 6 (2016).
5. G. Jeong, J. Kim, O. Gunawan, S.R. Pae, S.H. Kim, J.Y. Song, Y.S. Lee, B. Shin. Preparation of single-phase SnSe thin films and modification of electrical properties via stoichiometry control for photovoltaic application. *J. Alloys and Comp.* **722**, 474 (2017).

6. E.V. Kuchis. *Galvanomagnetic Effects and Methods of Their Studies* (Radio i Svyaz, 1990) (in Russian).
7. P. Blood, J.W. Orton. Methods for measuring the electrical properties of semiconductors. *Zarubezh. Radioelektr.* **1**, 2 (1981) (in Russian).
8. V.L. Mironov. *Fundamentals of Scanning Probe Microscopy* (Technosfera, 2004) (in Russian).
9. A.A. Radzig, B.M.Smirnov. *Parameters of Atoms and Atomic Ions* (Energoatomizdat, 1986) (in Russian).

Received 02.07.19

Дж.І. Хусейнов, Х.А. Хасанов,
Т.А. Джафаров, І.І. Аббасов

КОМПЕНСУЮЧА ДІЯ ДОМІШКИ ТЕРБІЮ
НА ПРОВІДНІСТЬ ТВЕРДИХ РОЗЧИНІВ $Tb_xSn_{1-x}Se$

Р е з ю м е

Досліджено взаємодії в системі SnSe–TbSe, і визначено область розчинності TbSe в SnSe за результатами комплексного фізико-хімічного аналізу. Проаналізовано залежність провідності і концентрації носіїв струму в $Tb_xSn_{1-x}Se$ кристалах від складу і температури.